One-Step Synthesis of Polycrystalline Carbon Nanofibers with Periodic Dome-Shaped Interiors and Their Reversible Lithium-Ion Storage Properties

Da Deng[†] and Jim Yang Lee*[,†,‡]

Department of Chemical & Biomolecular Engineering, Faculty of Engineering, National University of Singapore, 10 Kent Ridge Crescent, Singapore 119260, and Singapore−MIT alliance, National University of Singapore, 4 Engineering Drive 3, Singapore 117576

Received March 15, 2007. Revised Manuscript Received May 4, 2007

Carbon nanofibers and carbon nanotubes continue to draw unwavering interest from industrial and academic communities because of their fascinating properties and their projected application values. This paper reports a one-step synthesis of high-purity carbon nanofibers with dome-shaped interiors by the noncatalytic thermal decomposition of acetylene over a copper surface at atmospheric pressure. These uniquely shaped carbon nanofibers were impurity free, and their dome-shaped interiors could be repeated with high periodicity throughout the length. In addition, Y-junction and forklike carbon nanofibers with the same internal structure were also formed as byproducts. The growth of these unique carbon nanomaterials could be rationalized by a mechanism based on the autocatalytic chemical vapor deposition of 3D graphene flakes. Preliminary electrochemical measurements indicated that the carbon nanofibers could be used as the active anode material for lithium-ion batteries, delivering good cyclability and a reversible capacity of ∼260 mAh/g at the high specific current of 100 mA/g.

1. Introduction

The discovery of carbon nanotubes (CNTs) in 1991, followed by reports of their fascinating chemical, physical, and electronic properties, has enthralled the research community worldwide.[1,2] Current efforts are focused on the CNT fabrication techniques and the exploration of their morphology-related properties.[1−8] Among the synthesis methods known to date including arc-discharge,[1] templated deposition,[4] laser ablation,[5] and catalytic chemical vapor deposition (CVD),[6] catalytic CVD using various carbon precursors and Co, Fe, or Ni nanoparticle catalysts is the most common and scalable method to produce CNTs.[6] However, catalytic CVD is a multistep process involving catalyst preparation, CNT formation, and CNT purification. The CNTs prepared by catalytic CVD often contain residual catalyst particles and other carbon phases as impurities.[6−9] The purification step not only lowers the yield of CNT production but may also damage the CNT structure. From the practical standpoint, a simple one-step synthesis of high-purity CNTs without a purification step is always desirable.[31]

Besides the well-known single-wall and multiwall CNTs, other special forms of CNTs such as bamboolike CNTs,[10,11,25] conelike CNTs,[3] and Y-junction CNTs[12−15] have also been reported. Bamboolike CNTs had been synthesized by catalytic CVD using iron nanoparticles as the catalyst,[25] and more recently by the pyrolysis of organometallic precursors at high temperatures and pressures.[10] The Y-junction CNTs are receiving increasing attention because of their projected utility in future nanoelectronic devices and circuits.[12−15]

* To whom correspondence should be addressed. E-mail: cheleejy@nus.edu.sg.
[†] Department of Chemical & Biomedical Engineering, National University of Singapore.
[‡] Singapore−MIT alliance, National University of Singapore.

(1) Iijima, S. *Nature* **1991**, *354*, 56.
(2) Baughman, R. H.; Zakhidov, A. A.; de Heer, W. A. *Science* **2002**, *297*, 787.
(3) Zhang, G. Y.; Jiang, X.; Wang, E. G. *Science* **2003**, *300*, 472.
(4) Lee, J. S.; Gu, G. H.; Kim, H.; Jeong, K. S.; Bae, J.; Suh, J. S. *Chem. Mater.* **2001**, *13*, 2387.
(5) Thess, A.; Lee, R.; Nikolaev, P.; Dai, H.; Petit, P.; Robert, J.; Xu, C.; Lee, Y. J.; Fisher, J. E.; Smalley, R. E. *Science* **1996**, *273*, 483.
(6) Oncel, C.; Yurum, Y. *Fullerenes, Nanotubes, Carbon Nanostruct.* **2006**, *14*, 17.
(7) Chen, X. H.; Chen, C. S.; Chen, Q.; Cheng, F. Q.; Zhang, G.; Chen, Z. Z. *Mater. Lett.* **2002**, *57*, 734.
(8) Tobias, G.; Shao, L. D.; Salzmann, C. G.; Huh, Y.; Green, M. L. H. *J. Phys. Chem. B* **2006**, *110*, 22318.
(9) Murphy, R.; Coleman, J. N.; Cadek, M.; McCarthy, B.; Bent, M.; Drury, A.; Barklie, R. C.; Blau, W. J. *J. Phys. Chem. B* **2002**, *106*, 3087.
(10) Shanmugam, S.; Gedanken, A. *J. Phys. Chem. B* **2006**, *110*, 2037.
(11) Lee, C. J.; Park, J. *Appl. Phys. Lett.* **2000**, *77*, 3397.
(12) Gan, B.; Ahn, J.; Zhang, Q.; Yoon, S. F.; Rusli; Huang, Q. F.; Yang, H.; Yu, M. B.; Li, W. Z. *Diamond Relat. Mater.* **2000**, *9*, 897.
(13) Valles, C.; Perez-mendoza, M.; Castell, P.; Martinez, M. T.; Maser, W. K.; Benito, A. M. *Nanotechnology* **2006**, *17*, 4292.
(14) Li, J.; Papadopoulos, C.; Xu, J. *Nature* **1999**, *402*, 253.
(15) Gothard, N.; Daraio, C.; Gaillard, J.; Zidan, R.; Jin, S.; Rao, A. M. *Nano Lett.* **2004**, *4*, 213.
(16) Bandaru, P. R.; Daraio, C.; Jin, S.; Rao, A. M. *Nat. Mater.* **2005**, *4*, 663.
(17) Claye, A. S.; Fischer, J. E.; Huffman, C. B.; Rinzler, A. G.; Smalley, R. E. *J. Electrochem. Soc.* **2000**, *147*, 2845.
(18) Baibarac, M.; Lira-Cantu, M.; Oro-Sole, J.; Casan-Pastor, N.; Gomez-Romero, P. *Small* **2006**, *2*, 1075.
(19) Sharon, M.; Hsu, W. K.; Kroto, H. W.; Walton, D. R. M.; Kawahara, A.; Ishihara, T.; Takita, Y. *J. Power Sources* **2002**, *104*, 148.
(20) Wang, Y.; Lee. J. Y.; Zeng, H. C. *Chem. Mater.* **2005**, *17*, 3899.
(21) Ma, L.; Chen, W. X.; Xu, Z. D.; Xia, J. B.; Li, X. *Nanotechnology* **2006**, *17*, 571.
(22) Singh, C.; Shaffer, M. S. P.; Windle, A. H. *Carbon* **2003**, *41*, 359.
(23) Murakami, H.; Kirakawa, M.; Tanaka, C.; Yamakawa, H. *Appl. Phys. Lett.* **2000**, *76*, 1776.
(24) Saito, Y. *Carbon* **1995**, *33*, 979.
(25) Li, D. C.; Dai, L. M.; Huang, S. M.; Mau, A. W. H.; Wang, Z. L. *Chem. Phys. Lett.* **2000**, *316*, 349.

10.1021/cm0707206 CCC: $37.00
Published on Web 07/24/2007

Y-junction CNTs have been synthesized by template-assisted catalytic CVD using nanochanneled alumina as the template and Co as the catalyst.[14] Alternatively, Ti-doped Fe may also be used as the catalyst.[15]

Many of the so-called "CNTs" in the literature, including some of the references cited above, were actually carbon nanofibers (CNFs). This is because they either lacked the long-rang order of a perfect graphite structure or their graphene sheets were not rolled into perfect cylinders. CNFs could indeed be advantageous to some applications, such as using them as a reversible Li^+ storage material for the anode of lithium-ion batteries.[2,17−19] Here, the monolithic tubular structure of perfectly graphitized CNTs with few surface defect sites would limit Li^+ diffusion only through the opened ends of the CNTs. By comparison, Li^+ could diffuse more easily through the surface discontinuities in the walls of CNFs to result in increased Li^+ storage capacity at normal charge and discharge rates.

We report here a simple one-step CVD method to synthesize high-purity ultralong polycrystalline CNFs with periodic dome-shaped interiors. This method of preparation provides a number of advantages over the catalytic CVD methods.[6] High-purity ultralong CNFs with periodic dome-shaped interiors could be produced easily and harvested without the need for transition metal nanoparticle catalysts and purification posttreatments. The CNFs were collected on a copper substrate, which could be recycled. In addition, Y-junction and forklike CNFs with the same internal structure were formed as byproducts without any template or catalyst. The dome-shaped interiors were spaced uniformly throughout the length of the CNF and along the stem and branches of the Y-junction. The formation of CNFs with periodic dome-shaped interiors could not be satisfactorily rationalized by the base-growth or tip-growth models for hollow CNF formation by catalytic CVD processes. A new growth mechanism based on the autocatalytic deposition of 3D graphene flakes was therefore proposed. The CNFs were evaluated as an active anode material for reversible Li^+-ion storage. Preliminary results were encouraging as capacities in excess of 250 mAh/g could be realized without any pretreatment.

2. Experimental Section

CNF Preparation. In a typical experiment, a quartz combustion boat containing pure copper wires was placed in a tube furnace and heated at 950 °C for 3−6 h in a stream of 10% acetylene in nitrogen flowing at 200 sccm. The tube furnace was then allowed to cool to room temperature naturally in flowing nitrogen. A thick layer of black deposit was formed on the copper substrate, indicating the successful growth of the CNFs. No purification posttreatment was applied to the synthesized CNFs.

Material Characterizations. The CNFs were characterized by field-emission scanning electron microscopy (FESEM) and scanning transition electron microscopy (STEM) on a JEOL JSM-6700F operating at 5 and 25 kV respectively, scanning electron microscopy (SEM) and energy-dispersive X-ray spectroscopy (EDX) on a JEOL JSM-840 operating at 15 kV, transmission electron microscopy (TEM) on a JEOL JEM-2010F operating at 200 kV, high-resolution TEM (HRTEM) and selected area electron diffraction (SEAD) on a Philips FEG-CM300 operating at 200 kV, powder X-ray diffraction (XRD) on a Shimadu XRD-6000 using Cu Kα radiation, and Raman spectroscopy on a Jobin-Yavon T6400 micro-Raman system with Ar^+ laser at an excitation wavelength of 514.5 nm.

Electrochemical Measurements. The CNFs were mixed with 10% polyvinylidene fluoride (PVDF) binder in *N*-methylpyrrolidone (NMP) to form a homogeneous slurry. The slurry was applied over a copper disc current collector and dried in a vacuum at 120 °C overnight. Electrochemical test cells were assembled in an argon-filled glove box using a lithium metal foil as the counter electrode and 1 M $LiPF_6$/EC+DMC (1:1 w/w) as the electrolyte. The cells were tested on a Maccor Series 2000 battery tester at ambient conditions using a fixed charge and discharge current density of 100 mA/g in the voltage window 5 mV to 2 V.

3. Results and Discussion

The FESEM images of the black deposit on copper wires after 3 h of reaction are shown in Figure 1a−c at different magnifications. The low-magnification FESEM image (Figure 1a) shows that a large number of ultralong CNFs with a millimeter-length scale could be produced by this method of preparation. The preparation method could be easily scaled up for larger-quantity production and the copper metal substrate could be recycled. Images a and b of Figure 1 also show that the synthesized CNFs were free from foreign impurities, unlike the case of CNFs or CNTs prepared by other methods.[6,7,19,31] The CNFs had uniform diameters ranging from 100 to 200 nm and a smooth exterior. There was some repeating ripplelike contrast (boxed in Figure 1b for easy identification) lengthwise, which became more prominent in the zoomed-in view of Figure 1c. The ripplelike contrast was an indication of the periodic changes in carbon density along the length. These repeated patterns were also confirmed by TEM (vida infra). Figure 1d shows a looped-back CNF prepared with 6 h of CVD. The greater than 180° bending indicates that the CNFs had good mechanical properties.[10]

The most unique feature of these CNFs was their dome-shaped interiors, which were spaced uniformly throughout the length with high periodicity. The TEM images of the CNFs synthesized with 3 h of CVD on copper wires in Figure 2a−c show clearly the periodic dome-shaped interiors and the smooth outer surface. Some slightly bent CNFs indicating good ductility were again found in Figure 2a. The low-magnification TEM image Figure 2a also shows the high quality of the CNFs: there was no visible foreign matter. EDX analysis did not detect any copper metal in the CNFs produced (see Figure 5 in the Supporting Information). On the contrary, CNTs produced from typical catalytic CVD methods often contain catalytic metal nanoparticles at the tip or near the base of the CNTs, or carbon phase impurities (e.g, carbon particles), making the purification of those CNTs an essential but difficult step.[6,22−25,31] The current method

(26) Ajayan, P. M.; Nugent, J. M.; Siegel, R. W.; Wei, B.; Redlich, P. K. *Nature* **2000**, *404*, 243.
(27) Levesque, A.; Binh, V. T.; Semet, V.; Guillot, D.; Fillit, R. Y.; Brookes, M. D.; Nguyen, T. P. *Thin Solid Films* **2004**, *464−465*, 308.
(28) Wang, Z. L.; Kang, Z. C. *J. Phys. Chem.* **1996**, *100*, 17725.
(29) Chen, W. X.; Lee, J. Y.; Liu, Z. L. *Carbon* **2003**, *41*, 959.
(30) Xing, W.; Bai, P.; Li, Z. F.; Yu, R. J.; Yan, Z. F.; Lu, G. Q.; Lu, L. M. *Electrochim. Acta* **2006**, *51*, 4626.
(31) Grobert, N. *Mater. Today* **2007**, *10*, 28.

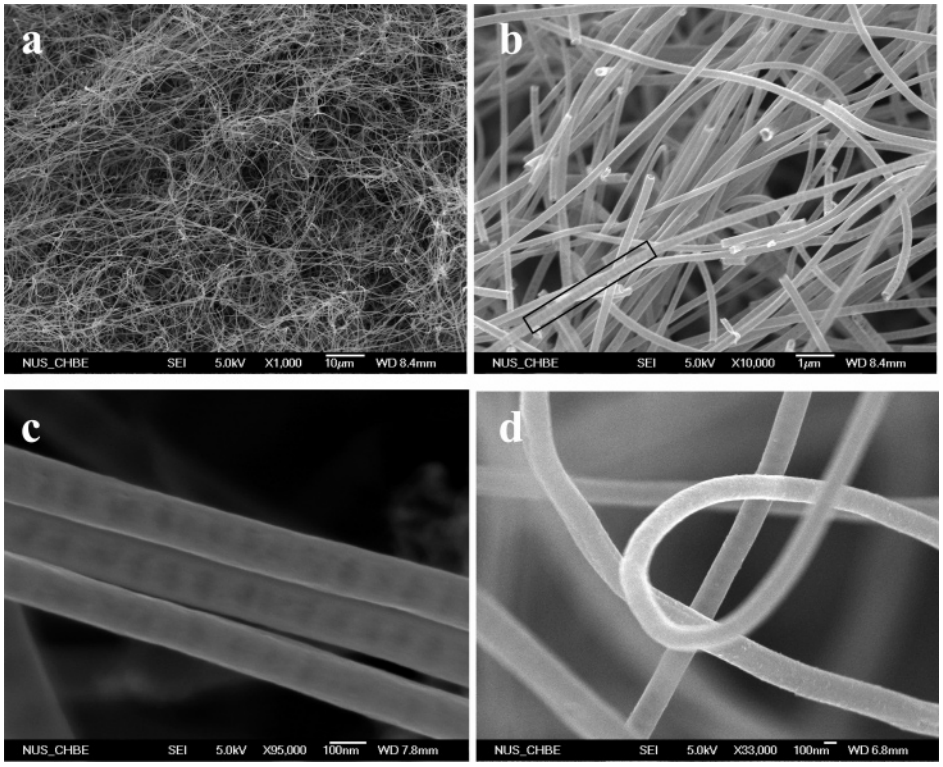

Figure 1. (a) Low-magnification and (b) high-magnification FESEM images of the CNFs; FESEM images of (c) three CNFs with ripplelike contrast along their lengths and (d) a looped-back CNF. CVD time: (a−c) 3 h, (d) 6 h.

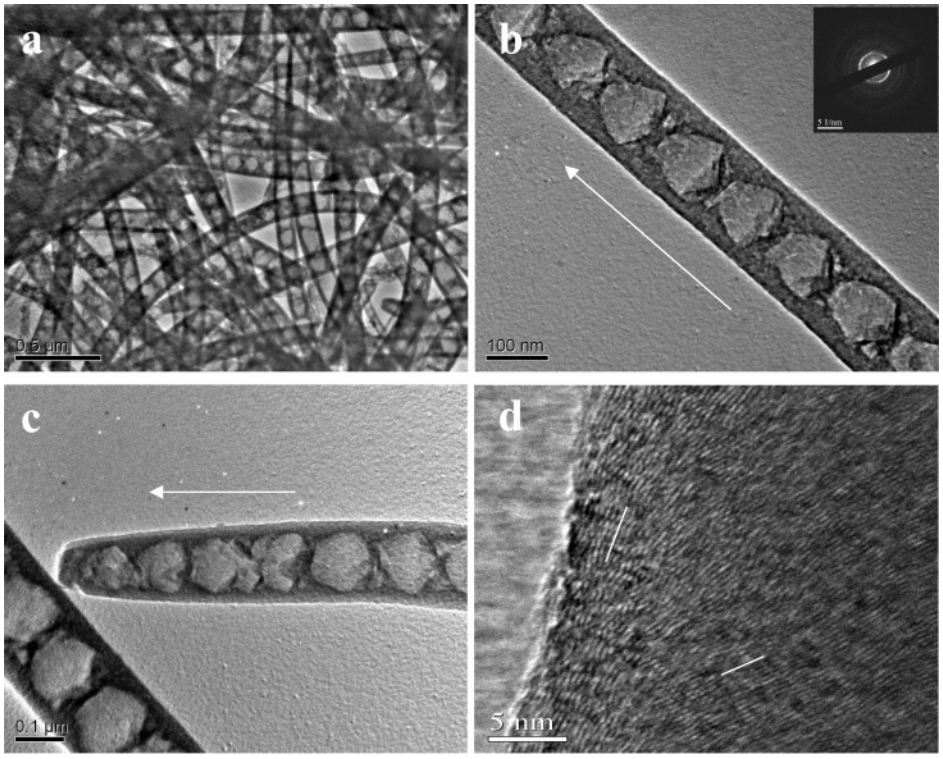

Figure 2. (a) Low-magnification TEM image of the CNFs. (b) High-magnification TEM image of a section of a typical CNF; the insert shows a typical SEAD pattern of the CNF. (c) TEM image of the tip of a typical CNF; the arrows in (b,c) show the growth direction of the CNFs. (d) Typical HRTEM image of the side of a CNF. The white lines in (d) show the direction of the aligned graphene sheets. CVD time: (a−d) 3 h.

of preparation suffers no such propensity. Figure 2b shows a typical section of the CNF with a more clearly revealed internal structure. The interiors contained well-separated dome-shaped cavities uniformly distributed along the CNF length. The arrows in the figure indicate that the growth direction was from the base of the dome to the apex. Figure 2c shows the catalyst-free tip of a single CNF, which was considerably different from CNTs produced by the tip-growth mechanism.[24]

Some Y-shaped and forklike CNFs, again with the periodic dome-shaped interiors, were also formed as byproducts. To the best of our knowledge, these intriguing morphologies

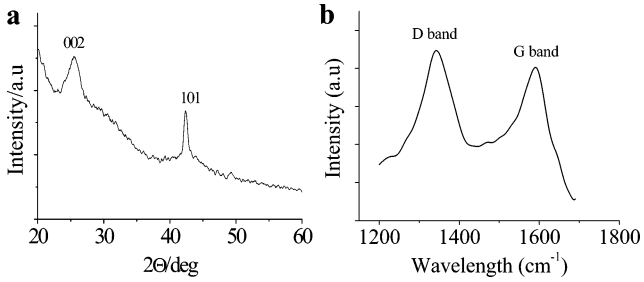

Figure 3. (a) XRD pattern and (b) Raman spectrum of the CNFs.

have not been previously observed. Some Y-junction CNFs with distinctive periodic dome-shaped interiors from 3 h of CVD on copper wires are shown in images a and b of Figure 4. Figure 4a shows two long branches sprouting from a common trunk. On the other hand, Figure 4b shows a Y-junction CNF with a prematurely terminated short branch. Although the Y-junction CNFs were difficult to separate from other CNFs, discovery of a template-free and catalyst-free synthesis leading to products with intriguing internal structures here is exciting nonetheless. If the Y-junction CNFs could be produced at higher yields with more precise morphology control, their use as the building blocks for nanoelectronics may be possible.[13] Images c and d in Figure 4 show that the forklike CNFs had the same periodic dome-shaped internal structure. Figure 4c shows a forklike CNF with two short branches departing from the stem at different junctions. On the other hand, Figure 4d shows a forklike CNF with three long branches diverging from the same junction. The formation of the forklike CNFs could be considered as an extension of the Y-junction growth with an additional third branch. This further confirmed the CNF growth direction was from the base of the dome to the apex as highlighted by the arrows in the figures. Clearly, the growth of catalyst-free Y-junction and forklike CNFs could not be satisfactorily explained by the popular base-growth model either.[11]

The formation of the CNFs was independent of the form of the copper substrate, i.e., copper wires, copper sheets, and copper TEM grids (see Figure 1 in the Supporting Information) all led to almost the same products. However, the CNFs grown on the copper TEM grid were somewhat rougher, which could be due to the presence of a carbon film in the TEM grid. On other substrates, such as KS6 graphite and quartz combustion boats, solid carbon wires were the only 1D product (see Figure 2 in the Supporting Information) and the amount formed was small when compared to the yield of CNFs on copper. It may therefore be concluded that a copper substrate was necessary for the formation of CNFs

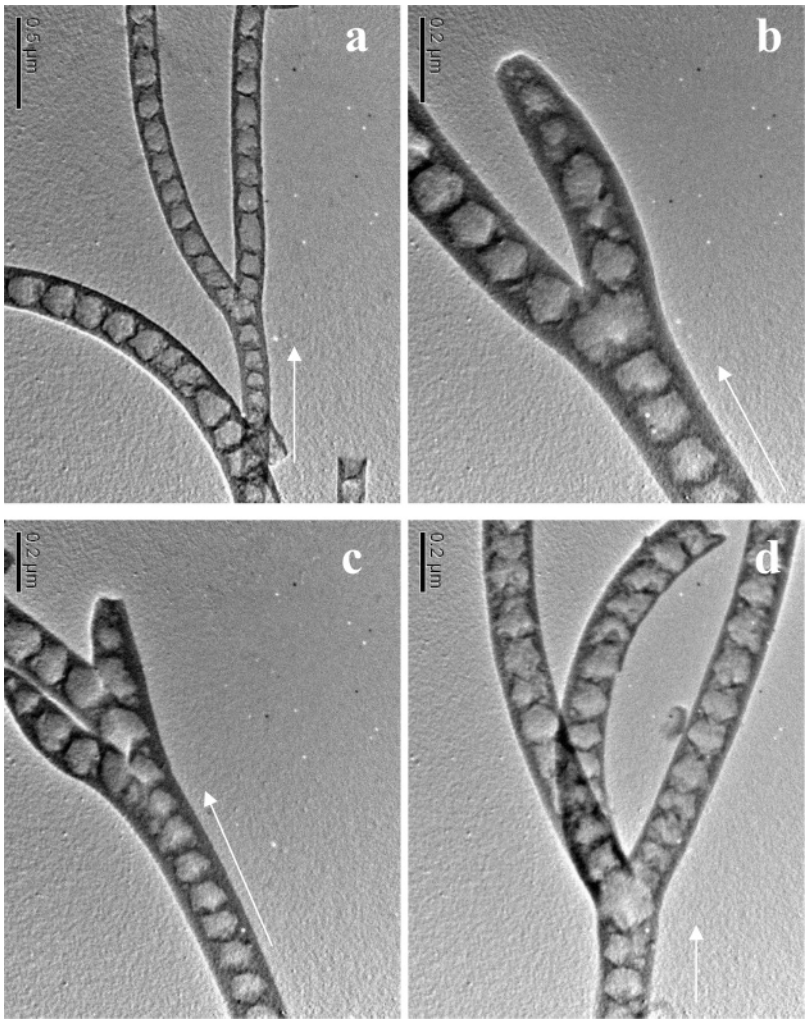

Figure 4. TEM images of the Y-junction CNFs: (a) with two long branches extending from a common junction; (b) with one short branch. TEM images of the forklike CNFs: (c) with two short branches; (d) with three long branches. The arrows in (a−d) show the growth direction of the CNFs. CVD time: (a−d) 3 h.

with dome-shaped interiors. There was no apparent effect of time on the CNF diameter, as shown by the FESEM images of CNFs synthesized by 6 h of CVD (see Figure 3 in the Supporting Information) vs those by 3 h of CVD. However, a longer CVD time did result in more CNFs being formed, and possibly longer CNFs, although the exact length was difficult to determine by FESEM because of the extra long length and the bends in the CNFs. On the contrary, the effect of temperature on the CNFs growth was strong and prominent. Experimentally, no CNFs were formed at temperatures below 700 °C. The CNFs formed at 850 °C (see Figure 4 in the Supporting Information) had a noticeably rougher exterior compared to the CNFs synthesized at 950 °C and broken holes (highlighted by arrows) were found on some of the CNFs.

The CNFs formed on copper were characterized by Raman spectroscopy. The resulting spectrum in Figure 3b shows strong D and G lines at ca. 1343 and 1587 cm^{-1}, respectively. The broadening of the lines into bands suggested that the CNFs had low crystallinity and were composed of small graphene sheets with a low degree of graphitization. The D band at 1343 cm^{-1} could be associated with structural defects and disorders in the CNFs. The G band at 1587 cm^{-1} was due to the vibration of sp^2-bonded carbon in a 2D hexagonal lattice, i.e., C═C bond stretching. Compared to pure graphite, which has only a sharp G band at around 1580 cm^{-1}, the prominent D band (1343 cm^{-1}) in Figure 3b indicated a low graphitization degree and the presence of a large quantity of defects and disorders. The 7 cm^{-1} shift in the G band of the CNFs (1587 cm^{-1}) relative to that of graphite (1580 cm^{-1}) is further evidence for the low graphitization degree of the graphene sheets in the CNFs.

To understand the possible growth mechanism for these unique CNFs, the crystallinity of the CNFs was carefully examined. The X-ray diffraction (XRD) pattern of the CNFs synthesized with 3 h of CVD is shown in Figure 3a. The diffraction peaks at ~25.5 and ~42.4° could be assigned to the (002) and (101) diffractions of graphitic carbon, respectively. The d_{002} calculated from the Bragg equation was 3.5 Å, which is slightly larger than that of graphite with d_{002} of 3.4 Å. The crystallite size based on the Scherrer equation ($D_v = K\lambda/\beta\cos\theta$, where $K = 0.9$, β is half width of the (002) peak, and $\lambda = 0.154$ nm) was 4.2 nm. The small crystallite size and the expanded d_{002} indicate that the CNFs had low crystallinity compared to graphite. The inset in Figure 2b shows a typical selected area electron diffraction (SAED) pattern of the CNF, where the absence of discrete diffraction spots indicates that the CNF was polycrystalline carbon. The HRTEM image of the walls of the CNF (Figure 2d) revealed that the CNF consisted of closely packed graphene sheets about 2−5 nm in length. Some of the graphene sheets were slightly curved and some graphene sheets contained both curved and straight sections. The interlayer distance d_{002} between the graphene sheets was measured to be ~3.6 Å on the average, in reasonably good agreement with the XRD determination (3.5 Å). These measurements are consistent with the results of Raman spectroscopy. The low graphitization degree could be due to the presence of curved, bent, and structurally imperfect

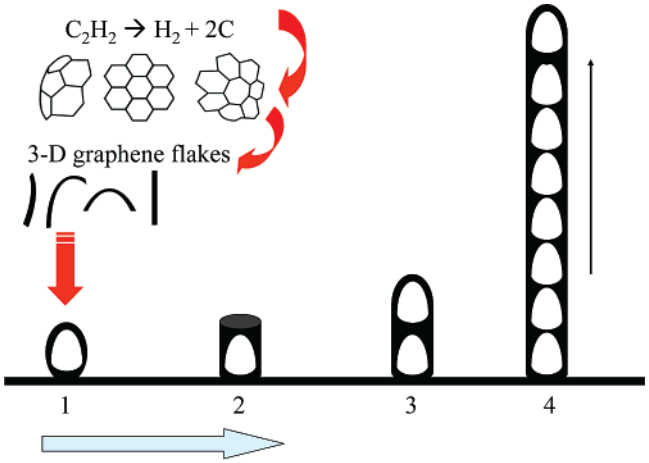

Figure 5. Proposed growth mechanism of the CNFs with periodically dome-shaped interiors.

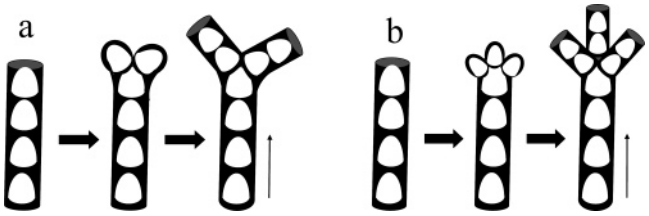

Figure 6. Proposed growth mechanism of (a) the Y-shaped and (b) fork-shaped CNFs with periodically dome-shaped interiors.

graphene sheets and the nonparallel arrangement of the wrinkled graphene sheets. The graphene sheets near the external surface were slightly inclined to the surface, whereas the graphene sheets away from the external surface were inclined at a larger angle to the CNF surface. Indeed, the graphene sheets above the dome-shape interiors were nearly perpendicular to the external surface (see Figure 6 in the Supporting Information).

The well-known tip-growth and base-growth mechanisms are unable to rationalize the growth of these unique CNFs. A new mechanism which incorporated the current views in the literature is proposed here as an alternative.[24,26−28] The new mechanism may be called autocatalytic 3D graphene flake deposition, where 3D graphene flakes refer to curved, bent, flat, rolled, and wrinkled graphene sheets. We perceived the growth of CNF to consist of the following events:

(1) Carbon from the gas-phase decomposition of C_2H_2 condensed and self-assembled into hexagonal, pentagonal, and heptagonal rings.[26−28] The rings combined to form small 3D graphene flakes about 2−5 nm in size (pyrolitic graphite structure), which are the basic construction units for the growth of a wire or tubular structure.[26−28]

(2) During the deposition of the 3D graphene flakes on the copper surface where carbon is insoluble,[24] the intrinsic curvatures of these surfaces promoted shape-conforming stacking, forming spherulites in a thin graphite layer (see Figure 7 in the Supporting Information).[26] (Step 1 in Figure 5). These spherulites were often found in the growth of 1D carbon nanostructures.[26]

(3) The spherulites were catalytic toward C_2H_2 decomposition, and more 3D graphene flakes were formed heterogeneously. The 3D graphene flakes had strong anisotropy[32] and were inclined to grow in directions that would help to extend

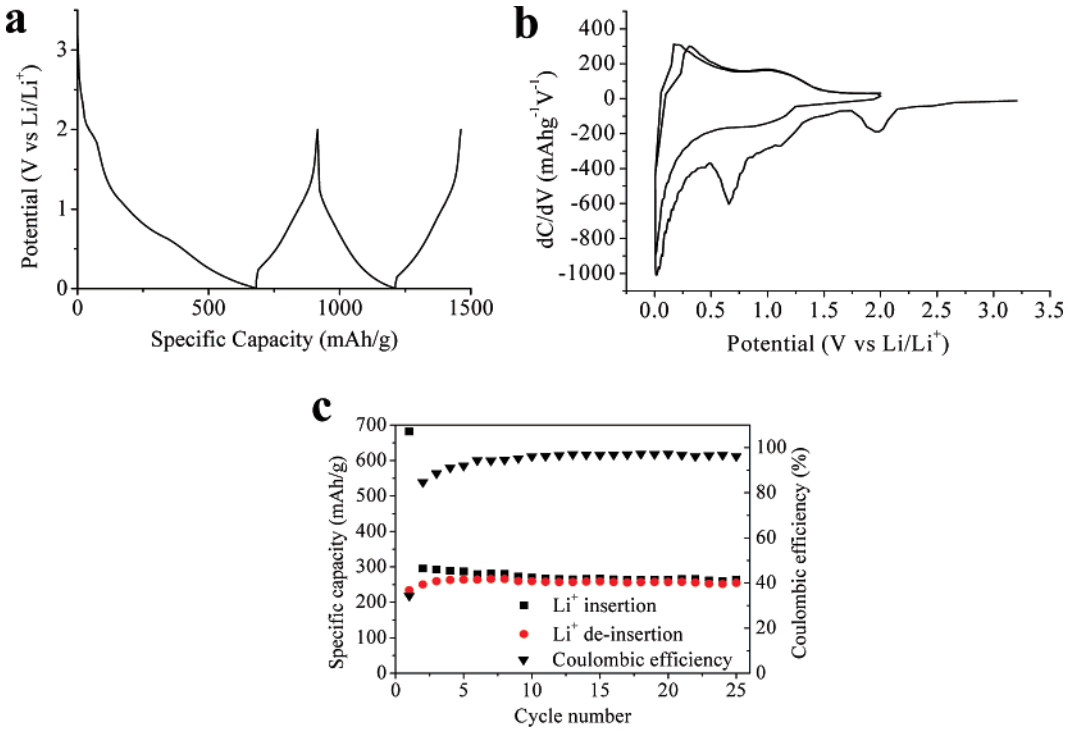

Figure 7. (a) Charge−discharge curves and (b) differential capacity plot of the CNF electrode for the first two cycles; (c) cycling performance and coulombic efficiency of the CNF electrode at a specific current of 100 mA/g.

their surfaces. The vertical alignment of the rolled surfaces would result in growth propagation in the CNF axial direction; in the mean time, some rolled surfaces stacked to form the tube walls (Step 2 in Figure 5).

(4) The autocatalytic process also produced curved surfaces that grew internally with increasing angles of inclination to the CNF axis (see the HRETM images in Figure 2d in text and Figure 6 in the Supporting Information). When the growth was extensive enough, the tube opening was closed with the formation of a tip, signaling the closure of a "section" (Step 3 in Figure 5).

(5) The tip of the section then assumed the original role of the spherulites, and the growth process repeated. (Step 4 in Figure 5).

The exact role of copper is not known at present. Phenomenonlogically, copper promoted the formation of an initial carbon film with spherulitic character, which stimulated the outward growth of 1D tubular structures.

The formation of the Y-shaped and forklike CNFs could also be understood on the basis of the mechanism of directed deposition of 3D graphene flakes (Figure 6). The formation of Y-shaped CNF (see images a and b in Figure 4) could be the result of the overdeposition and aggregation of 3D graphite flakes on a CNF tip, resulting in the formation of two graphene spheres pointing in different directions. The two carbon nanospheres could then serve as independent autocatalytic sites and nuclei to seed the directed aggregation and deposition of 3D graphene flakes, creating the Y-junction with periodically dome-shaped interiors shown in Figure 6a. The two branches could be competing for graphene flake deposition, leading to the asymmetric growth of the two branches (see Figure 4b). Similarly, the formation of forklike CNFs could be explained by the mechanism shown in Figure 6b, where three carbon nanospheres on the same part of the stem (Figure 4d) seeded the growth of the branches of the fork.

Measurements of the reversible lithium-ion storage property of the CNFs were carried out to evaluate the suitability of the CNFs in lithium-ion battery applications. Figure 7a shows the first two cycles of charging (Li^+ insertion) and discharging (Li^+ deinsertion) the CNF electrode. The voltage plateau at about 0.7 V in the first charging cycle is normally associated with electrolyte decomposition and the formation of a solid electrolyte interface (SEI). A very large lithium-ion storage capacity of 682 mAh/g was obtained in the first charging cycle, of which 234 mAh/g could be recovered upon the first discharge. The large irreversible capacity loss (∼65%) was contributed not only by SEI formation but also by the reduction of oxygen species present on the CNF surface.[29,33] Indeed, the presence of a trace amount of oxygen in the CNFs was confirmed by EDX analysis (Figure 5 in the Supporting Information). In addition, some lithium ion could be "trapped" at void or cavity sites by the "ink-bottle" effect, compounding the first cycle irreversible capacity losses.[35] Large first cycle irreversible capacity losses had been witnessed for CNTs prepared by the catalytic CVD method using Co nanoparticles.[33] A differential capacity plot (dC/dV vs potential, Figure 7b) based on Figure 7a was used to accentuate the features in the Li^+ insertion and extraction processes. In this regard, the peaks at ∼0.7 and ∼2 V in the

(32) Tenne, R. *Angew. Chem., Int. Ed.* **2003**, *42*, 5124.
(33) Wang, G. X.; Ahn, J.; Yao, J.; Lindsay, M.; Liu, H. K.; Dou, S. X. *J. Power Sources* **2003**, *119*−*121*, 16.
(34) Rosolen, J. M.; Matsubara, E. Y.; Marchesin, M. S.; Lala, S. M.; Montoro, L. A.; Tronto, S. *J. Power Sources* **2006**, *162*, 620.
(35) Chevallier, F.; Gautier, S.; Salvetat, J. P.; Clinard, C.; Frackowiak, E.; Rouzaud, J. N.; Beguin, F. *J. Power Sources* **2001**, *97*−*8*, 143.

first charging cycle corresponded well with SEI formation and the reduction of surface oxygen on CNFs, respectively. As these were first cycle processes, they disappeared expectedly in the second and subsequent cycles. During the discharging process, a broad anodic peak common to graphite and CNF electrodes was found at ~0.25 V,[19,29,30] which may be used to infer that the CNFs had certain graphitic character. The reversible Li^+ storage capacity and coulombic efficiency of the CNF electrode were plotted as a function of the cycle number in Figure 7c. Except for the first cycle, where the large irreversible capacity loss weighed down the coulombic efficiency to a low of ~35%, a coulombic efficiency of ~97% was possible from the second cycle onward. A reversible Li^+ storage capacity of ~260 mAh/g was sustainable, indicating reasonably good cyclability of the CNF electrode. It should be pointed out that the CNF electrode was tested in the 5 mV to 2 V window at a relatively high rate of 100 mA/g, and yet its performance surpassed the previously reported value of CNTs (100 mAh/g) tested at the same current density and in a wider voltage window (0.01−3.0 V).[33] The test electrode was formulated without a conductivity enhancer such as Super P carbon black, indicating that the CNFs were intrinsically highly conductive. Although the measured reversible Li^+ storage capacities were higher than the typical values for CNTs,[19,29,33,34] they have yet to match the capacity of graphite (372 mAh/g with LiC_6 stoichiometry). The better than average capacity of our CNFs could be attributed to their polycrystalline character, which allowed Li^+ diffusion through the walls and be stored in the interstices between the graphene sheets. However, as the CNFs still had a fairly thick shell, efficient Li^+ storage in the dome-shaped interiors was likely not well-accomplished.

4. Conclusion

In summary, CNFs with periodic dome-shaped interiors were synthesized by the one-step chemical vapor decomposition of acetylene over copper surfaces at atmospheric pressure. The CNFs were unique in that they were relatively impurity free and their dome-shaped interiors were regularly spaced throughout the CNF length. In addition, hitherto undiscovered Y-junction and forklike CNFs with periodic dome-shaped interiors were formed as one of the byproducts. A new growth mechanism based on the autocatalytic deposition of 3D graphene flakes was proposed. The cyclability of these CNFs in reversible Li^+ storage was quite good, with a reversible capacity of ~260 mAh/g realizable at the rate of 100 mA/g. In principle, the CNFs with periodic dome-shaped interiors could be used to template other nanoarchitectures or to form nanocomposites by coating or diffusing other material precursors into the gaps of the graphene sheets via gas-phase or liquid-phase processes. Some of these activities are currently being pursued in our laboratory.

Supporting Information Available: EDX pattern and HRTEM images of the typical CNFs grown on copper wires by 3 h CVD at 950 °C; FESEM images of CNFs grown on a TEM copper grid and on a copper sheet; FESEM images of CNFs synthesized by 6 h of CVD at 950 °C; FESEM images of CNFs synthesized by 5 h of CVD at 850 °C (PDF). This material is available free of charge via the Internet at http://pubs.acs.org.

CM0707206